This article was downloaded by: [216.179.31.22]
On: 18 April 2013, At: 08:39
Publisher: Taylor & Francis
Informa Ltd Registered in England and Wales Registered Number: 1072954 Registered office: Mortimer House, 37-41 Mortimer Street, London W1T 3JH, UK

Aerosol Science and Technology
Publication details, including instructions for authors and subscription information:
http://www.tandfonline.com/loi/uast20

Improved Method for the Evaluation of Real-Time Biological Aerosol Detection Technologies

Shanna Ratnesar-Shumate [a b], Michael L. Wagner [a], Charles Kerechanin [a], Gerad House [a], Kelly M. Brinkley [a], Christopher Bare [a], Neal A. Baker [a], Rachel Quizon [a], Jason Quizon [a], Alex Proescher [a], Eric Van Gieson [a] & Joshua L. Santarpia [a b]

[a] National Security Technology Department, The Johns Hopkins University Applied Physics Laboratory, Laurel, Maryland, USA

[b] Department of Civil and Environmental Engineering, The University of Maryland Baltimore County, Baltimore, Maryland, USA

Version of record first published: 06 Feb 2011.

To cite this article: Shanna Ratnesar-Shumate , Michael L. Wagner , Charles Kerechanin , Gerad House , Kelly M. Brinkley , Christopher Bare , Neal A. Baker , Rachel Quizon , Jason Quizon , Alex Proescher , Eric Van Gieson & Joshua L. Santarpia (2011): Improved Method for the Evaluation of Real-Time Biological Aerosol Detection Technologies, Aerosol Science and Technology, 45:5, 635-644

To link to this article: http://dx.doi.org/10.1080/02786826.2010.551144

PLEASE SCROLL DOWN FOR ARTICLE

Full terms and conditions of use: http://www.tandfonline.com/page/terms-and-conditions

This article may be used for research, teaching, and private study purposes. Any substantial or systematic reproduction, redistribution, reselling, loan, sub-licensing, systematic supply, or distribution in any form to anyone is expressly forbidden.

The publisher does not give any warranty express or implied or make any representation that the contents will be complete or accurate or up to date. The accuracy of any instructions, formulae, and drug doses should be independently verified with primary sources. The publisher shall not be liable for any loss, actions, claims, proceedings, demand, or costs or damages whatsoever or howsoever caused arising directly or indirectly in connection with or arising out of the use of this material.

Aerosol Science and Technology, 45:635–644, 2011
Copyright © American Association for Aerosol Research
ISSN: 0278-6826 print / 1521-7388 online
DOI: 10.1080/02786826.2010.551144

Improved Method for the Evaluation of Real-Time Biological Aerosol Detection Technologies

Shanna Ratnesar-Shumate,[1,2] Michael L. Wagner,[1] Charles Kerechanin,[1] Gerad House,[1] Kelly M. Brinkley,[1] Christopher Bare,[1] Neal A. Baker,[1] Rachel Quizon,[1] Jason Quizon,[1] Alex Proescher,[1] Eric Van Gieson,[1] and Joshua L. Santarpia[1,2]

[1]*National Security Technology Department, The Johns Hopkins University Applied Physics Laboratory, Laurel, Maryland, USA*

[2]*Department of Civil and Environmental Engineering, The University of Maryland Baltimore County, Baltimore, Maryland, USA*

Downloaded by [216.179.31.22] at 08:39 18 April 2013

There is a growing need to evaluate bioaerosol sensors under relevant operational conditions. New methods are needed that can mimic the temporal fluctuations of ambient aerosol backgrounds and present biological aerosol challenges in a way that simulates a plausible biological agent attack. The Dynamic Concentration Aerosol Generator was developed to address this need. The authors developed a series of aerosol challenges consisting of *Bacillus thuringiensis kurstaki* (*Btk*) spores in the presence of background aerosols using a newly developed ramp testing method. Using ramping style tests, 5-min *Btk* releases were overlaid on top of a background aerosol that fluctuated at varying rates. Background aerosol compositions for different tests were designed to simulate the types of aerosol in the ambient environment. Background aerosol concentration was varied between 7.0×10^3 and 1.5×10^4 particles per liter of air (ppL). Aerosol number concentrations of *Btk* for the challenges were approximately 2.5×10^3 ppL and the culturable fraction of the collected *Btk* aerosol was estimated to be 1.25×10^3 colony forming-units (cfu)/L-air. Results of these experiments demonstrate a novel technique for dynamic aerosol generation that can be used to test biological aerosol sensors under controlled conditions designed to reproduce observed fluctuations in the ambient aerosol.

INTRODUCTION

The need to rapidly identify weaponized pathogenic biological aerosols before symptoms manifest in host populations is critical to protecting military forces and domestic populations. This concern has led to the development of a variety of sensors to detect the full spectrum of aerosolized biological threats including spores, bacteria, viruses, and toxins. Detecting biological warfare agents in real time is difficult. Many non-biological particles and chemical vapors that may be present in the environment can interfere with detection technologies (Vandenberg 2000; Carrano et al. 2005). Pathogenic organisms that cause disease in humans may be chemically and physically very similar to a wide range of other largely innocuous atmospheric particles of biological origin.

Ivnitski et al. (2005) suggest that biological detection systems should consist of a network of instruments that incorporate two types of sensors: portable detectors, also referred to as "triggers," that alert users to the presence of a biological attack; and more sophisticated sensors that identify the specific bacteria, virus, or biological toxin present in the air. Optical sensors, based on spectroscopic techniques, are obvious candidates for trigger systems. They can measure biological aerosol concentrations at very rapid rates (seconds to minutes), quickly alerting the user to a potential threat (Ivnitski et al. 2005; Samuels et al. 2006; Vanderberg 2000). However, these sensors have not been shown to discriminate between different types of microorganisms and may also incorrectly identify certain non-biological aerosol particles as a threat. Several different types of optical detection technologies, including fluorescence spectroscopy, vibrational spectroscopy, and transduction methods have been investigated (Vanderberg 2000). The most common type of optical biological sensor utilizes spectroscopic autofluorescence or light-induced fluorescence (LIF) (Wilson and Defreeze 2003; Schroder et al. 1999; Eversole et al. 2001; Hill et al. 1999; Tilley et al. 2001). Systems using LIF technology detect fluorescent compounds present in most biological materials including tryptophan, nicotinamide adenine dinucleotide plus hydrogen (NADH), and flavins. The spectroscopic signal detected by a sensor is dependent upon the wavelength used to excite the molecules in the particle, as well as the relative ratios of signature compounds within the biological species being

Received 20 February 2010; accepted 14 November 2010.
Address correspondence to Joshua L. Santarpia, National Security Technology Department, The Johns Hopkins University Applied Physics Laboratory, 11100 Johns Hopkins Rd., Laurel, MD 20723, USA. E-mail: joshua.santarpia@jhuapl.edu

Downloaded by [216.179.31.22] at 08:39 18 April 2013

interrogated. In many cases, light scattering from a particle is also used to infer size and shape information. The operation of these non-specific biological detection systems can be dramatically affected by the natural fluctuations in the ambient background of biological aerosol. Misidentification of biological threats in these instances may require expensive identification tests for collected samples, evacuation of facilities, unnecessary use of personal protective equipment, and eventual complacency to electronic detections that are actually true (Vanderberg 2000; Samuels et al. 2006; Carrano et al. 2005).

The background aerosol encountered in the ambient environment contains naturally occurring biological aerosols that may fluctuate according to meteorological conditions, biological processes, or other factors (Lighthart and Shaffer 1995; Shaffer and Lighthart 1997). High temporal resolution data of changes in total respirable aerosol and biological aerosol are only available in limited cases. Tilley et al. (2001) showed significant fluctuations in the biological aerosol concentration over a period of 4 days at two outdoor sites in Australia using LIF measurements of single aerosols and bioaerosol collection systems. The ratio of biological aerosols consisting of bacteria and fungi to the total aerosol count was shown to vary significantly. Total aerosol counts were shown to range from 2246 to 5708 ppL with the absolute rates of change ranging from 1.05 to 15.51 ppL/min. The percent of bacteria and fungi present in the total aerosol counts was estimated to range from 1.5% to 5.1% for bacteria and 1.5% to 2.0% for fungi.

Due to the potential operational impacts, it is critical to understand how the response of a biological aerosol detector sensor is affected by fluctuations in the ambient environment. Ideally, sensor testing would occur in operationally relevant environments (Carrano et al. 2005). Factors such as the geographical location and meteorological conditions can affect the performance capability of a sensor. Transportation, cost, and logistical difficulties associated with field testing—particularly when it is desirable to reproduce a threat-like aerosol—creates a need to re-create realistic field conditions within a laboratory setting to pre-screen developmental technologies. Additional testing with live bacteria or pathogenic agents in an outdoor setting is limited by cost and the potential threat posed to surrounding populations. To effectively evaluate the potential performance of a sensor in an operational environment, the laboratory test must attempt to accurately reproduce the ambient aerosol compositions, concentrations, and temporal profiles to those in which the sensor is required to operate, while delivering threat-like aerosol challenges to evaluate both the detection capability and the ability to reject fluctuations in the ambient background.

Test and evaluation of biological aerosol detection systems typically occurs in several phases. Initially, it is important to understand the sensitivity of the sensor to both threat-like challenges and to ambient or background aerosol. Sensors may be tested under conditions where the concentration of a challenge aerosol (biological agent or agent simulant) or background aerosol particles is increased from virtually no particles (<1 ppL) to high concentrations of aerosols ($\sim 10^3$ ppL) (Semler et al. 2004; Ho 1989; Ho et al. 2001). This can measure the fundamental sensitivity of the sensor to an aerosolized material, but it does not directly evaluate how a sensor might perform in the field. Another level of evaluation incorporates a constant background aerosol concentration, such as a dust, non-biological material, or mixtures of biological and non-biological aerosol, against which a challenge material is generated (Wilson and Brady 2004). This type of test requires an aerosol wind-tunnel or continuous-flow aerosol delivery system; it allows the evaluation of sensor performance against a simple background, but it does not capture natural fluctuations in the ambient aerosol that may affect sensor performance. To better re-create natural fluctuations in biological and non-biological aerosol concentrations, a novel aerosol test system was developed. The Dynamic Concentration Aerosol Generator (DyCAG) provides a means for sensor system evaluation by generation of simulant challenges at specific concentrations in the presence of various levels of environmentally relevant aerosols using a unique aerosol generation and test system. By utilizing the dynamic capability of the DyCAG system in combination with measured ambient data, test scenarios can be re-created in a contained laboratory setting that provides simulated ambient conditions for sensor evaluation. The DyCAG can generate up to seven independent aerosols, four of which can vary in concentration independently, before combining and mixing in an airstream for delivery to sensors under test.

In this work, the capability of the DyCAG system to generate a background aerosol within a controlled laboratory setting that fluctuates similar to those observed from outdoor measurements is demonstrated. Biological agent simulant challenges are then overlaid above these background aerosols to exhibit how this testing technique could be used to evaluate biological sensors in a realistic test environment.

MATERIALS AND METHODS

Aerosol Test System

The DyCAG (Figure 1) consists of three main control regions: an aerosol generation and injection region, a mixing region, and an isokinetic sampling region. The DyCAG aerosol generation and injection region can combine aerosols from up to four ultrasonic generators and two aerosol materials from Collison nebulizers (Table 1) and the exhaust of a diesel engine. Individual aerosol components are generated and conditioned independently from one another and then mixed to form the desired complex imitation of an ambient environmental aerosol mixture.

To allow newly generated aerosols time to dry (if necessary) and to allow the concentration of aerosol to become consistent before it is introduced into the DyCAG flow stream, Aerosol Capacitance Chambers (ACCs; Figure 2) are used to divert aerosol before it enters the DyCAG. The ACC provides a reservoir of high-concentration aerosol from a single source that can then

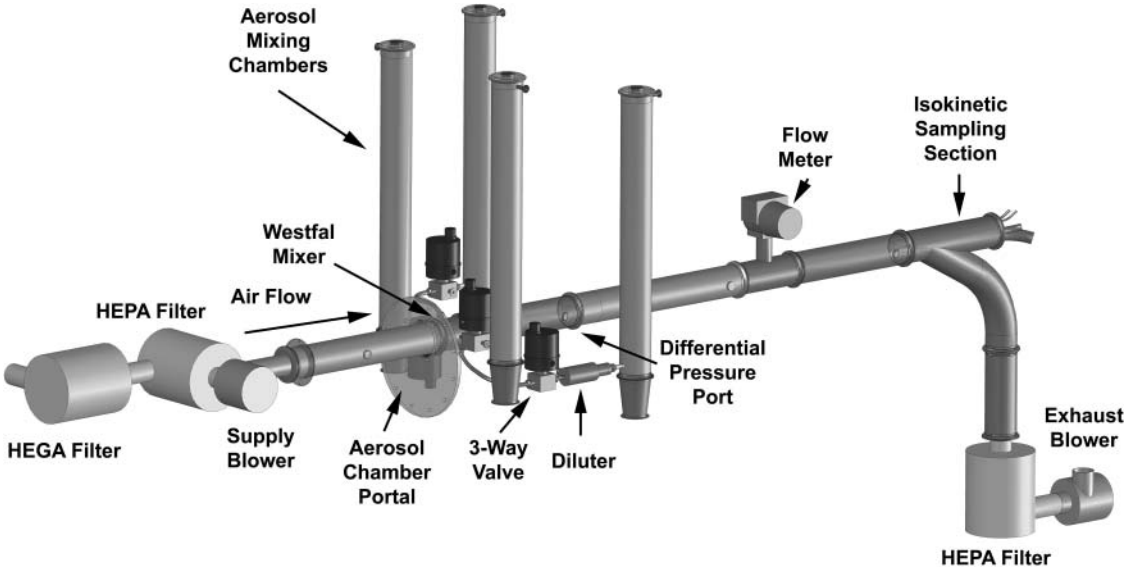

FIG. 1. Overview of Dynamic Concentration Aerosol Generator (DyCAG) showing the different components that make up the DyCAG system.

Downloaded by [216.179.31.22] at 08:39 18 April 2013

be metered into the bulk airflow and mixed with aerosols from other sources.

Sono-Tek ultrasonic atomizers are used for aerosol generation and are the primary source of aerosols for the DyCAG system. Liquid is fed to the Sono-Tek nozzle (Table 1) using a dual-feed syringe pump (Table 1). A Broadband Ultrasonic Generator (BUG) (Table 1) generates high-frequency vibrations that disrupt the liquid flow at the nozzle tip and atomize the liquid. These atomizers allow for the discrete control of the injection rate of aerosol mass into the ACC and do not increase the air pressure within the ACC. The dry particle size of the aerosols generated by the Sono-Tek is controlled by the concentration of the solute in the liquid being atomized (Hinds 1999). By varying the rate of liquid injection, the amount of material generated can be modified and used to control the concentration of material introduced into the test chamber. Droplets generated by the Sono-Tek require drying time before introduction to the mixing region to allow solvent evaporation. The ACC design uses the Sono-Tek nozzles pointing downward into the capacitance chamber, parallel to a flow of dry compressed air entering the ACC at flow rates variable between 1 and 15 Lpm (Figure 2a).

TABLE 1
DyCAG Components

No.	Part	Model No.	Manufacturer
1	Nozzle	06–04010	Sono-Tek Corporation, Milton, NY
2	Dual-feed Syringe Pump	11–01061	Sono-Tek Corporation, Milton, NY
3	Broadband Ultrasonic Generator (BUG)	06–05108	Sono-Tek Corporation, Milton, NY
4	Collison 3-Jet Nebulizer	CN24	BGI Inc., Waltham, MA
5	Filtered Air Supply	3076	TSI Inc., Shoreview, MN
6	Injection Mixer	—	Westfall Manufacturing Co., Bristol, RI
7	Blowers	119105E	Ametek Inc., Paolie, PA
8	Flow Meter	600–9	Thermal Instrument Co., Trevose, PA
10	Mass Flow Controller	FMA 5400–5500	Omega Engineering Inc., Stanford, CT
9	Omega X Differential Pressure Sensor	PX653–2.5BD5V	Omega Engineering Inc., Stanford, CT
10	Ultraviolet Aerodynamic Particle Sizer (UVAPS)	3314	TSI Inc, Shoreview, MN
11	All-glass Impingers	7540	Ace Glass Inc., Vineland, NJ
12	Autoplate 4000 Spiral Plating System	4000	Spiral Biotech, Inc.
13	QCount System Colony Counter	—	Spiral Biotech, Inc.

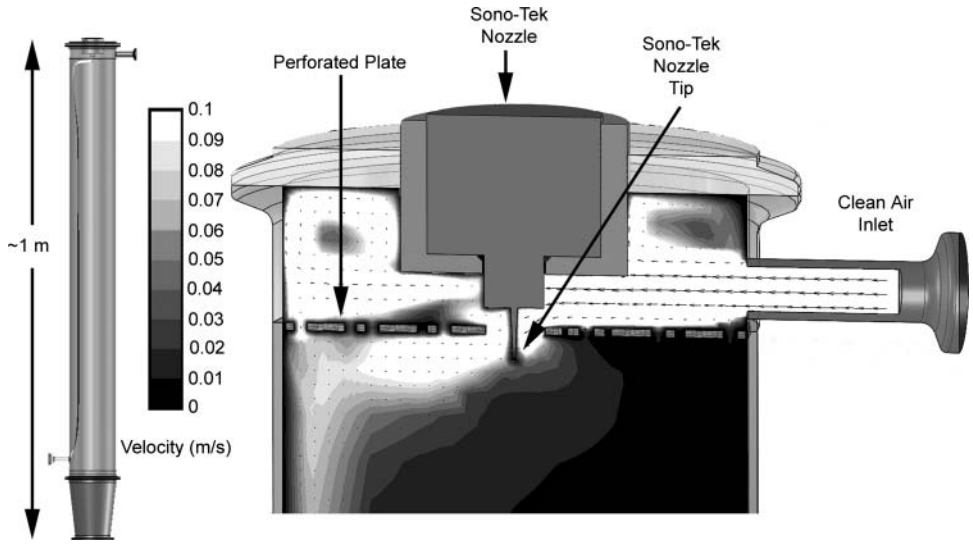

FIG. 2. Computational fluid dynamics simulation of final ACC Design. (a) CFD analysis shows that 5 μm particles generated via Sono-Tek are introduced at the top of the ACC and have approximately 55 s of drying time when the air inlet is at 5.0 Lpm. Particles greater than 30 μm fall to the bottom of the ACC to prevent carryover and non-aerosolize liquid from entering into the DyCAG. (b) Velocity profile of aerosol generation using Sono-Tek nozzles orientated vertically in the ACC.

Downloaded by [216.179.31.22] at 08:39 18 April 2013

To produce a well-controlled aerosol within the ACC, the source of the liquid being delivered to the nozzle must be a well-mixed suspension of material. A stir bar is placed within the syringe and a magnetic stir plate is held in place above the syringe to mix the suspension before it is pumped to the nozzle. Computational fluid dynamics (CFD) simulations, using Cosmos FloWorks (Structural Research and Analysis Corp., Los Angeles, California) of the ACC show that a 5 μm particle has approximately 55 s of drying time when the compressed air inlet is at 5.0 Lpm. According to the model, particles 30 μm or greater will fall to the bottom of the ACC, out of the airflow, preventing carryover between runs. In this way, non-aerosolized liquid from the Sono-Tek nozzles and agglomerated particles larger than 30 μm are collected at the bottom of the ACC, while the test aerosol travels down the ACC and exits through the small tube in the side of the wall with sufficient time to dry.

A Collison 3-Jet nebulizer (Table 1) can be used to generate a background aerosol that does not pass through an ACC. Clean, dry particle free air is supplied directly to the Collison nebulizer using a filtered air supply (Table 1) at 20 psi. The Collison nebulizer is attached to a mini-stir bar plate running at full speed with a 1-inch stir bar placed inside the nebulizer reservoir to maintain the suspension and minimize settling of the material to the bottom of the container.

Aerosols are uniformly mixed with filtered air using a modified Westfall injection mixer (Westfall Manufacturing Co., Bristol, RI). The injection module consists of a modified orifice with injection ports situated just downstream of the Westfall mixer (Figure 1). Computational models from Cosmos FloWorks (not shown) indicate that the velocity profile across the tube is uniform and that 1 μm aerosol particles introduced at the injection ports are mixed throughout the cross-section at 10 tube diameters downstream of the mixing element. Two Ametek blowers (Table 1) are used to provide the bulk mixing flow in the DyCAG system. Air is drawn from the room through a high-efficiency particulate air (HEPA) filter and a high-efficiency gas abatement (HEGA) filter to remove particulate and gasses that may complicate the test process. Flow is exhausted through another HEPA filter to prevent the aerosolized test material from escaping into the surrounding laboratory. The peak airflow using this arrangement is $\sim$2500 Lpm, which allows for a wide variety of sensors and reference equipment to sample isokinetically and without influencing one another. Bulk flow is measured immediately upstream of the sensor sample location to ensure accurate measurement of the system flow and calculations of the volume concentration. A flow meter (Table 1) with a sampling inner diameter that equal that of the DyCAG delivery tube is used for flow measurement. This eliminates any additional parts that may protrude into the aerosol flow. An Omega X differential pressure sensor (Table 1) is used to set the system to an operating pressure of –0.1 in. H_2O to allow the DyCAG to perform as the primary aerosol containment barrier. The aerosol concentration and composition in the DyCAG delivery tube is controlled and varied by regulating the flow from each of the four ACCs with Omega mass flow controllers (Table 1).

Multiple biological detection systems can be tested simultaneously in the DyCAG, along with reference measurements, using isokinetic sampling probes for each unit to sample from the bulk flow after mixing (Figure 3). The designs of the sampling probes for each sensor or reference measurement are generated based on the cross-sectional air velocity of each sensor inlet (calculated from manufacturer-specified flow rate) against the

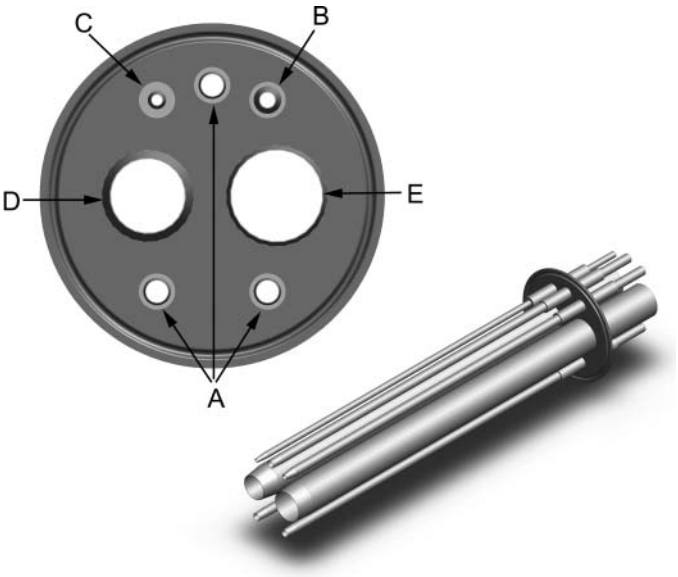

FIG. 3. Example DyCAG isokinetic sampling port. The inset image shows the arrangement of isokinetic sampling ports: three ports for reference filters or impingers (A: 9–12.5 lpm), a port for the UV-APS (B: 5 lpm), and several ports designed for other instrumentation that samples at a variety of flow rates (C: 1.5 lpm; D: 200 lpm; E: 400 lpm). The (A) ports were used to study the uniformity of aerosol in the DyCAG.

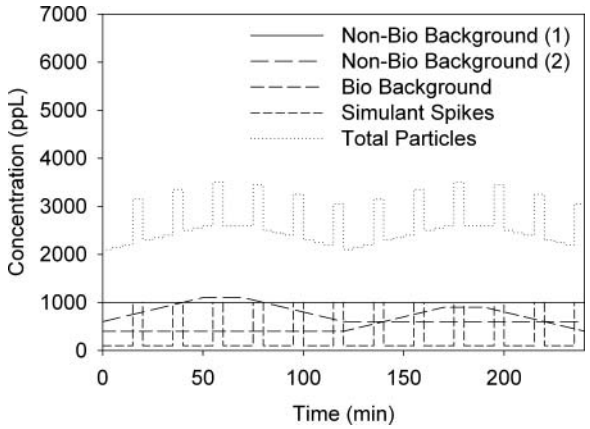

FIG. 4. Illustration of ramp aerosol challenges. The background material that ramped alternated from one ramp cycle to the next. During each 40-min cycle, sensors were exposed to two 15-min periods of background aerosol followed by a 5-min *Btk* challenge. The *Btk* challenges reach their peak concentration in 10 s and are maintained until the end of the 5-min challenge. By overlaying the *Btk* challenges throughout the ramp cycle, the sensors were challenged to detect simulant while the background was increasing, held constant, and decreasing.

Downloaded by [216.179.31.22] at 08:39 18 April 2013

entering air velocity of the DyCAG delivery system (2500 Lpm) to optimize particle sampling and to avoid any sensor-to-sensor bias (Baron and Willeke 2001). These calculations are used to predict the sampling tube size that will allow for the velocity at each sampling tube to be equal to the velocity in the mixing and delivery tube, which ensures that all sensors will sample the same aerosol concentrations. Inlet ends are tapered to knife-edges to minimize the frontal area of the sampling tubes. The cross-sectional area of the tube that is obstructed by the sampling probes during these experiments is approximately 20% of the cross-sectional area of the main airflow tube. Unsampled air continues past the sample probes and leaves the DyCAG main flow tube through a T-Y coupling into a HEPA filter (Figure 1).

SUMMARY OF EXPERIMENTS

The DyCAG was characterized to ensure that it could deliver well-mixed aerosol to multiple systems under test and referee systems. One SonoTek nebulizer was used to generate 3.1 μm green fluorescent polystyrene latex spheres (Catalog # GO300, Thermo Scientific, Waltham, MA) through one of the ACCs. This aerosol was sampled at three locations in the isokinetic sampling port (Figure 3) using Isopore filters with a 0.8 μm pore size (Catalog # ATTP04700, Millipore, Billerica, MA) sampling at 9 Lpm for 20 min, during 5 separate experiments. The filter flow rate was controlled continuously throughout the 20 min sampling using a flow controller (Model # MCR-250SLPM-D/5M, Alicat Scientific, Tucson, AZ). The filters were recovered by submerging each filter in 20 mL of 0.22 μm sterile-filtered deionized water (SFDI H_2O) in a 50 mL conical tube and placing it on an orbital shaker for 20 min. The fluorescence intensity of the beads in suspension was measured using a Trilogy 7200 fluorimeter (Turner Designs, Sunnyvale, CA). The mean and standard deviation of the fluorescence intensity from the three reference filters was calculated for each experiment. The standard deviations from each experiment indicate that the variation in aerosol concentration between the three locations was between 1.3% and 5.3%, with a mean of 3.1% for all 5 experiments. This demonstrates that aerosol particles are well mixed prior to sampling at the isokinetic ports.

A series of experiments were conducted that demonstrate the capabilities of the DyCAG system to recreate aerosol profiles with varying rates representative of outdoor aerosol. The repeatability of the ramp testing was evaluated for two series of the designed ramps. For these experiments, *Bacillus thuringiensis kurstaki* (*Btk*), a bacterium similar to *Bacillus anthracis*, was released into the DyCAG to simulate a biological release and to demonstrate the potential use of the DyCAG for evaluating the detection capabilities of biological sensors. The *Btk* spores were obtained directly from Dugway Proving Grounds (DPG), U.S. Army, Salt Lake City, Utah, and rehydrated at 10 mg/mL in SFDI H_2O for at least 24 h and stored at 4°C until ready for use.

The rates calculated from data reported in Tilley et al. (2001) are very slow ($\sim$10 ppL/min) and proved to be difficult to quantify reproducibly with the available reference equipment and sampling arrangement. Therefore, the ramps were designed to produce fluctuations in the test aerosol that are representative of the types of fluctuations observed in ambient aerosol but at rates that are more easily generated and measured in the DyCAG (Figure 4). A constant background aerosol of Arizona

TABLE 2
Background aerosol components and generation techniques

Testing description	Name	Concentration of stock material	Vendor information	Generation method
Constant background aerosol	Arizona Road Dust/$CaCO_3$	1 mg/mL	PTI, Catalog # ISSO 121031, A1	Sono-Tek
Non-bio background	Atlantic Sea Salt	Stock concentration	Sigma Aldrich, CAS 471–34—1 Atlantic Seawater, OSIL, UK	Sono-Tek
	Kaolin	0.5 mg/mL	Sigma Aldrich, Catalog # 1512	Sono-Tek
	Rayon Flock	0.5 mg/mL	WR200Z, International Fiber Corporation	Sono-Tek
Bio background	*Yersinia rhodei*	9.1E06 cfu/mL	American Type Culture Collection #43380	Sono-Tek
	Bacillus subtilis	1.0E7 cfu/mL	Dugway Proving Grounds	Sono-Tek
	Penicillium brevicompactum	1.1E6 spore/mL	Research Triangle Institute	Sono-Tek

Downloaded by [216.179.31.22] at 08:39 18 April 2013

Road Dust (ARD; Table 2) mixed in a 1:1 ratio with $CaCO_3$ aerosol was generated using one of the Sono-Tek nozzles. This mixture is intended to reproduce the ionic composition of dust collected in Saudi Arabia (U.S. Army Environmental Hygiene Agency 1994). Two other background aerosols, one biological and one non-biological, were ramped up and down. The non-biological background consisted of a mixture of Atlantic seawater, rayon flock, and kaolin (Table 2). The non-biological mixture is intended to represent other non-biological aerosol often found in the environment in areas of human activity such as sea-salt aerosol, material from clothing, and clay material that is prominent in many soils. The biological background aerosol consisted of Gram-positive *Bacillus subtilis* bacterial spores, *Penicillium brevicompactum* fungal spores, and Gram-negative *Yersinia rhodei* mixed in a ratio (∼50% gram-positive, ∼45% gram negative and ∼5% fungal; Table 2) that is representative of biological aerosol that has been collected in Laurel, MD (Santarpia et al. 2010). Initially dry materials were prepared for aerosolization by hydration in SFDI H_2O, at the concentrations listed in Table 2, and are mixed by vortex. After preparation, all materials are stored at 4°C until needed.

Each ramp cycle design consisted of 2 h experiments broken into 40-min cycles (Figure 4). During each 120-min ramp cycle, one of the background aerosols was held constant at the minimum concentration, while the other was increased over a 40 min period to the maximum concentration, held at the maximum concentration for a 40 min period, and ramped down to the minimum concentration for 40 min. The background material that ramped alternated from one ramp cycle to the next. Each 40 min cycle consisted of two 15-min periods of background aerosol followed by 5-min *Btk* challenges. The *Btk* challenges reached their peak concentration in 10 s and were maintained until the end of the 5-min challenge (Figure 4). By overlaying the *Btk* challenges throughout the ramp cycle, sensors could be challenged to detect simulant while the background is increasing, held constant, and decreasing. Each ramp experiment was repeated twice for demonstration of repeatability.

Controlling the compressed air flowrate for each ACC produces the fluctuations in aerosol concentration in the DyCAG. For this experiment the non-biological aerosol ramps were created by changing the compressed air flow rate linearly over a period of 40 min from 1 to 14 Lpm. After reaching the peak concentration, the flow rate was maintained at 14 Lpm for 40 min, and then ramped back down to 1 Lpm over a period of 40 min. The biological background flow rates were ramped from 1to 8 Lpm and back down to 1 Lpm in a pattern similar to the ramps described for the non-biological background.

Reference Measurements

Two instruments were used to quantify the aerosol challenges in the DyCAG. An Ultraviolet Aerodynamic Particle Sizer (UV-APS; Table 1) was used to quantify the aerosol concentration, aerodynamic size distribution, and fluorescent size distribution continuously with a sample time of 10 s. Reference samples were collected using sterile all-glass impingers (AGI-30; Table 1). The AGI-30s sampled the airflow at 12.5 Lpm into 20 mL of SFDI H_20. Samples were plated in triplicate on Tryptic Soy Agar via the Spiral Biotech Autoplate 4000 Spiral Plating System (Table 1) and then enumerated via the Spiral Biotech QCount System (Table 1). Samples with expected concentrations greater than 1.0×10^5 colony-forming units per milliliter (cfu/mL) were serially diluted with SFDI H_20 to achieve an approximate concentration of 1.0×10^3 cfu/mL and then plated. Plated samples were allowed to dry before they were inverted and incubated overnight (14–18 h) at 37°C. The average concentration (cfu/mL) of the three plates was reported for each sample. The starting volume in each AGI-30 was 20 ml of SFDI H_2O.

Downloaded by [216.179.31.22] at 08:39 18 April 2013

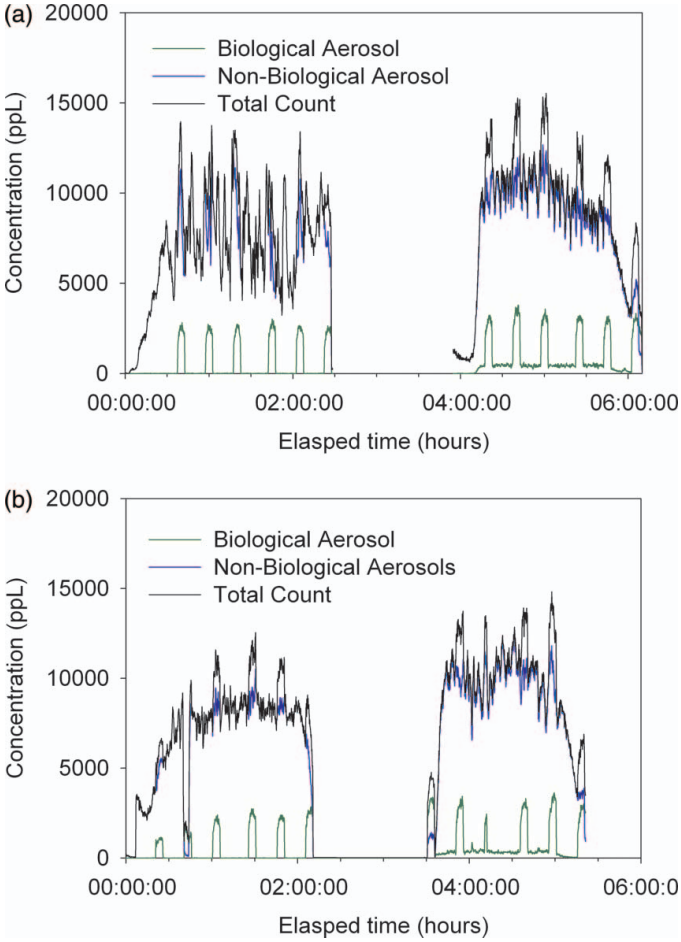

FIG. 5. Example of UV-APS data showing ramp experiments created using the DyCAG. The slash line trace depicts biological aerosol (relative fluorescence > 3), the solid line trace shows non-biological aerosol, the dotted line trace shows combined aerosol concentration. Two ramp cycles were performed per experiment. Two experiments were performed on different days are shown (a and b). The first ramp was created by changing the non-biological background while holding the biological background constant. During the second ramp, the biological background was ramped while the non-biological background remained constant. During each ramp six spikes of *Btk* were released. Between reach ramp cycle, the DyCAG aerosol is allowed to baseline to zero and then restarted. Approximately 45 min into the first ramp of the second experiment, communication between the DyCAG and the control computer was lost causing aerosol generation to stop briefly. (Figure provided in color online.)

RESULTS

A series of experiments were performed that demonstrated the ability of the DyCAG to generate dynamic aerosol populations that represented ambient aerosols populations in a controlled laboratory environment. Particle concentrations measured with the UV-APS during these experiments were comparable to particle counts observed by Tilley et al. (2001). By gating the fluorescence of particles measured in the UV-APS using a relative fluorescence value of 3 to discriminate between non-biological and biological particles (Huffman et al. 2010), the biological aerosol, the non-biological aerosol, and the combined aerosol concentrations were calculated and plotted (Figure 5). The actual total counts for both ramps 1 and 2 ranged from about 7×10^3 to 1.5×10^4 ppL with the average at approximately 7.8×10^3 ppL. For particles greater than 1 μm the range of total counts was from 6×10^3 to 1.2×10^4 ppL. During the second ramp of each experiment, the biological background was observed to contribute to an increase in the baseline biological aerosol concentration of particles greater than 1μm at about 4.3×10^3 ppL. By separating the two types of aerosols based on relative fluorescence, the *Btk* spikes were easily observed during each of the ramps. The *Btk* aerosol concentrations were measured by the UV-APS to be approximately 2.5×10^3 ppL for both experiments.

The UV-APS data indicated that the overall aerosol behavior in the DyCAG was consistent with the experiment design during both ramps on both days of experiments; however, the behavior of the aerosol over short timescales and apparent inconsistencies in the aerosol concentration, despite maintaining control over aerosol generation control parameters, were obvious from the data. Two primary features in the recorded UV-APS data indicated areas where control over the aerosol concentration in the background aerosol was problematic. Beginning around 1:45 h into the first ramp and at approximately the same time in the second ramp during the first day (5:45 h into the experiment; Figure 5a) there was an unplanned decrease in the aerosol concentration. During these periods, the operating parameters of the Sono-Tek nozzle remained the same and the rate of change of the airflow in the ACC remained consistent (Figure 6); however, in both cases the aerosol concentration in the DyCAG dropped unexpectedly (Figure 5a). This occurred again, to a lesser degree, during the biological ramp on the second day of experiments

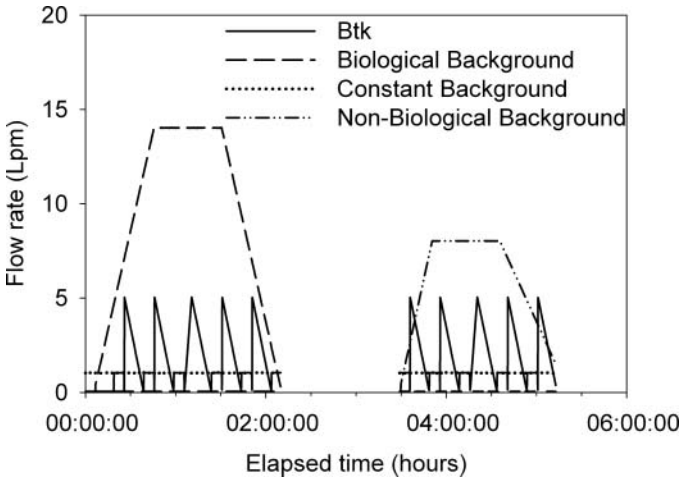

FIG. 6. Flow rates recorded for ACC carrier flow during the first of the two ramp experiments. Since the Sono-Tek aerosol generators are run with the same parameters into each ACC the aerosol concentration in the DyCAG from each ACC is controlled primarily by changing the flow rates. Note the small step function in flow rate in the *Btk* channel. This is used to clear out the ACC between challenges. During these periods, aerosol is sent out through a HEPA filter rather than through the DyCAG.

TABLE 3
Btk concentration determined by culture for ramp experiments (cfu/L-air)

Release number	Cycle 1	Cycle 2	Cycle 3	Cycle 4
1	3.05E + 01	1.07E + 03	1.31E + 03	4.57E + 02
2	1.65E + 03	1.07E + 03	1.99E + 03	8.88E + 02
3	1.07E + 03	1.26E + 03	2.17E + 03	7.62E + 02
4	1.92E + 03	1.19E + 03	3.36E + 03	1.25E + 03
5	1.62E + 03	9.78E + 02	7.35E + 02	1.07E + 03
6	1.86E + 03	9.46E + 02	1.07E + 03	7.31E + 02

at approximately hour 4:00 to 4:30 (Figure 5b). The reason for these unexpected changes was not apparent, but it may be due to changes in the uniformity of the suspension in the syringe (despite the continuous stirring of the suspension throughout the experiments). On the second day of experiments different anomalies were observed despite identical control parameters. During the second day (Figure 5b), there was an initial lag in the increase of background aerosol in both the non-biological and biological background ramps. Despite this, the shape of the non-biological ramp was more representative of the experimental design than the non-biological ramp during the first day. It was also notable that there were various spikes within the overall aerosol concentrations (Figure 5). These spikes appeared more prominent in the non-biological ramp than in the biological ramp during the first experiment (Figure 5a) and more prominent in the biological ramp during the second experiment (Figure 5b). This may indicate that the suspension used to produce the more irregular aerosol was less uniformly mixed in the syringe prior to aerosolization than the other one. The aerosol flow rate profiles (Figure 6) were virtually identical on both days of testing (not shown) indicating that the source of these anomalies is likely in the aerosol generation process. Spikes in aerosol concentrations are often observed in ambient data and while these spikes were not a part of the designed experiment, and compromise experimental reproducibility, they are consistent with the types of temporal variability in aerosol concentrations that are observed in the ambient environment.

The average *Btk* concentration for the 5 min challenges determined via culture of the samples collected with the AGI-30 during the ramp testing was $1.2 \times 10^3 \pm 5.1 \times 10^2$ during the first set of two ramps and $1.3 \times 10^3 \pm 8.2 \times 10^2$ cfu per L of air during the second set (Table 3). The *Btk* aerosol challenge concentrations were estimated from the AGI-30 samples by assuming a liquid evaporation rate from the impinger of 20.0–0.2t (where t = sampling time) for 5 min (Lin et al. 1997) a collection efficiency of 50% and a particle retention efficiency of 95% (Kesavan et al. 2010). The reported assay values account for these losses and are reported as the calculated airborne concentration of *Btk* for each challenge.

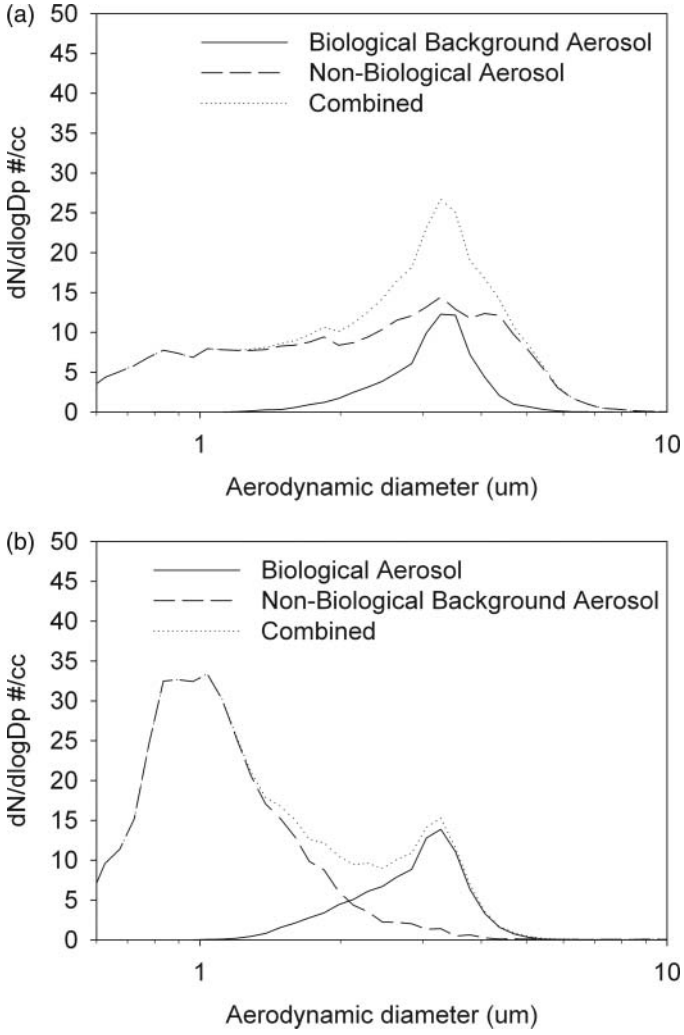

FIG. 7. Size distribution of aerosol particles while *Btk* was present during each type of ramp. Biological aerosol size distribution is shown in solid line trace and non-biological aerosol size distribution is shown in dash. (a) Size distributions for non-biological background ramp taken from the third Btk release of the first ramp during experiment the first experiment. (b) Size distribution for biological background ramp taken from the third Btk release of the second ramp during the second experiment.

The aerodynamic size distribution for the non-biological, biological, and combined distributions were generated by using the same gating of fluorescence for each ramp cycle (Figure 7). The size distribution of *Btk* aerosol, best represented by the first ramp of each experiment due to lack of other fluorescent particles, (Figure 7a) showed a peak size at approximately 3.3 μm. Given the ratio of culturable *Btk* to the UV-APS measured biological aerosol concentration and the physical size of bacterial spores of *Btk* ranging from 1.07–1.99 μm (Carrera et al. 2007), it was likely that the biological aerosols consisted of a mixture of multiple spores per particle, as well as dry media and buffer. It is also likely that as many as 50% of the fluorescent aerosol did not contain viable spores. When the biological

Downloaded by [216.179.31.22] at 08:39 18 April 2013

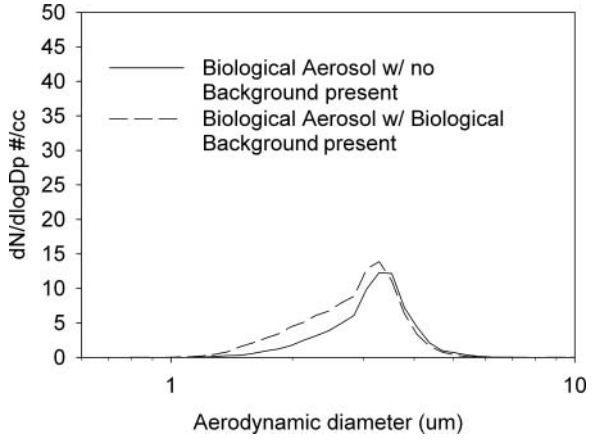

FIG. 8. Comparison of size distributions for biological aerosols with biological background present and absent. Biological distributions are overlaid from Figure 7 for comparison.

background was present at a high concentration during a ramp (Figure 7b, distribution recorded during the second ramp cycle of the first experiment) the biological aerosol size distribution showed a broad tail in the fine mode due to the presence of the biological background (a mixture of bacterial and fungal spores and bacterial cells). The non-biological portion of the aerosol is mono-modal with a peak ranging from 0.84 to 1 μm (Figure 7b). When the size distribution of biological aerosols with biological background present and absent is compared, a broader distribution is observable when the biological background is present with a larger concentration of particles occurring between 1 to 3 μm due to the presence of the biological background mixture (Figure 8).

Figure 9a–d shows a 10 s fluorescence distribution of each type of aerosol challenge, non-biological background, non-biological background when *Btk* is present, biological background, and biological background when *Btk* was present. In the case of the non-biological background ramp, when no *Btk* was present, a broad distribution of aerosols with multiple peaks was observed, the addition of *Btk*, shows a single mode biological component, but the non-biological background distribution remained relatively similar to the distribution observed in the absence of *Btk*. This suggests that biological fluorescence information could be used to discriminate between biological and non-biological aerosols, and allows for a semi-quantifiable measure of the biological aerosol component that may be correlated to other biological measurements techniques. For the second ramp, a broader distribution of the biological aerosols with a higher concentration of particles between 1 and 3 μm was present due to the biological background (Figure 7b). These particles are observable in the fluorescence distribution shown in Figure 9c when *Btk* was not present.

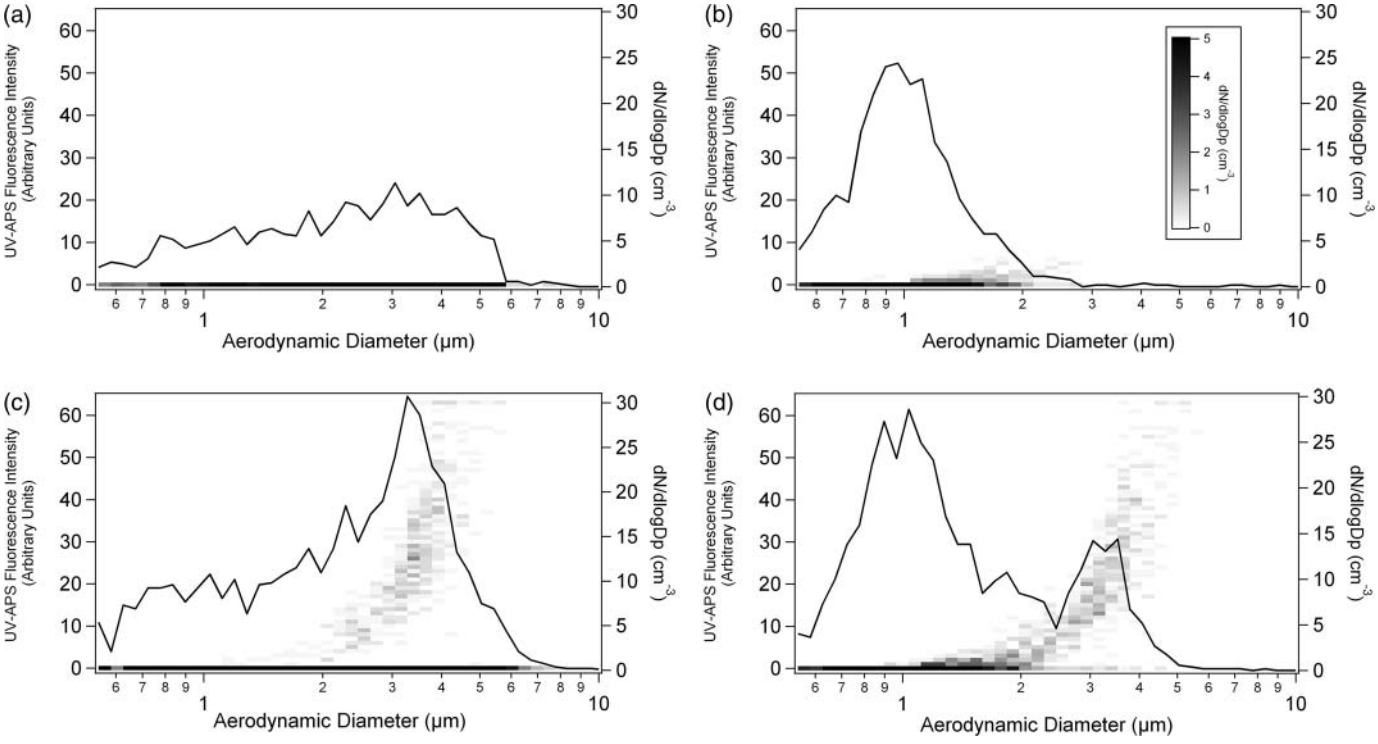

FIG. 9. Fluorescence properties (image plot) of aerosol during the first two cycles of ramps as measured by the UV-APS overlaid with the aerosol number distribution (black trace). (a) shows the size-resolved fluorescence and number distribution when only the non-biological background was generated, while (b) shows the same measurement when Btk was generated on top of this background aerosol. (c) shows the size-resolved fluorescence and number distribution when only the biological background was being generated, while (d) shows the same measurement when Btk was generated on top of this background aerosol.

Downloaded by [216.179.31.22] at 08:39 18 April 2013

Downloaded by [216.179.31.22] at 08:39 18 April 2013

SUMMARY AND DISCUSSION

The need to be able to protect military forces and domestic interests from the threat of biological weaponry is ever present in modern times. Various biological sensors have been developed that utilize multiple detection technologies to provide an alert to the presence of an aerosolized biological agent. Sensors need to be tested in a laboratory setting that is representative of the operationally relevant scenarios in which they are required to perform. Real-time information about ambient aerosol concentrations, size distributions, and chemical and biological makeup can be used to recreate these scenarios in a laboratory setting. A limited amount of this type of data has been generated that demonstrates the fluctuations of the aerosol populations. Traditional sensor testing is often static, consisting of pulse aerosol challenges with little to no manipulation of the background aerosol. In order evaluate the performance of biological sensors under conditions that are representative of real-world environments there exists a need to recreate ambient aerosols populations within a controlled laboratory setting. The DyCAG system is capable of generating a dynamic range of aerosols fluctuating in concentration and composition.

Ramping experiments, in which the background aerosol concentration was dynamic, were performed during two series of tests. Single particle biological fluorescence measurements and microbial culture were used to quantify the biological, nonbiological, and total aerosol concentrations during testing. These experiments demonstrated the ability to simulate representative ambient aerosol fluctuations within a controlled laboratory setting; however, improvements to the airflow control are need to exactly reproduce the slow rates of change that have been observed in available ambient datasets (Tilley et al. 2001). The apparent difficulty in maintaining the consistent aerosol generation needed to produce the background ramps for greater than 1.5 h demonstrates the need for improved methods for generating consistent aerosol over long periods. In addition, more detailed data on the composition, fluctuations, and biological diversity of ambient aerosol at various geographic locations and seasons is needed to build a stronger data set for experimental challenges. These datasets could be used to better define the shape and composition of fluctuations in laboratory test aerosols in order to provide more realistic backgrounds to evaluate emerging biological aerosol sensors in the laboratory.

REFERENCES

Baron, P. A., and Willeke, K. (2005). *Aerosol Measurement Principles, Techniques, and Applications*. John Wiley & Sons, New York, p. 1131.

Carrano, J., Jeys, T., Cousins, D., Eversole, J., Gillespie, J., Heally, D., Licata, N., Loerop, W., O'Keefe, M., Samuels, A., Schultz, J., Walter, M., Wong, N., Billote, B., Munley, M., Reich, E., and Roots, J. (2005). *Chemical and Biological Sensor Standards Study*. United States of America, Defense Advanced Research Projects Agency, Department of Defense. DTIC, Fort Belvoir, VA.

Carrera, M., Zandomeni, R. O., Fitzgibbon, J., and Sagripanti, J.-L. (2007). Difference Between the Spore Size of Bacillus anthracis and Other Bacillus Species. *J. Appl. Microbiol.* 102:303–312.

Eversole, J. D., Cary, W. K., Scotto, C. S., Pierson, R., Spence, M., and Campillo A. J. (2001). Continuous Bioaerosol Monitoring Using UV Excitation Fluorescence: Outdoor Test Results. *Field Anal. Chem. Technol.* 15(4):205–212.

Hill, S. C., Pinnick, R. G., Niles, S., Pan, Y.-L., Holler, S., Change, R. C., Bottiger, J., Chen, B. T., Orr, C.-S., and Feather, G. (1999). Real-Time Measurement of Fluorescence Spectra from Single-Airborne Biological Particles. *Field Anal. Chem. Technol. SI*. 3(4–5):221–239.

Hinds, W. C. (1999). *Aerosol Technology Properties, Behavior, and Measurement of Airborne Particles*. John Wiley & Sons, New York, p. 483.

Ho, J. (1989). Design of a Chamber for CBW Aerosol Studies with Relative Humidity and Particle Concentration Control. *Defense Res. Establishment.* Tech. no. AD-A205 623.

Ho, J., Spence, M., and Duncan, S. (2001). Live Biological Particle Measurement: Comparison of Slit Sampler Performance in a Biological Aerosol Chamber. *Defense Res. Establishment*. DRES TR 2001–139.

Huffman, J. A., Treutlein, B., and Poschl, U. (2010). Fluorescent Biological Aerosol Particle Concentration and Size Distributions Measured with an Ultraviolet Aerodynamic Particle Size (UV-APS) in Central Europe. *Atmos. Chem. Phys.* 10:3215–3233.

Ivintski, D., Morrison, D., and O'Neil, D. J. (2005). Critical Elements of Biological Sensor Technology for Deployment in an Environmental Network System, in *Defense Against Bioterrorism, Detection Technologies, Implementation Strategies, and Commercial Opportunities*. D. Morrison, F. Milanovich, D. Ivinitski, T. R. Austin, eds., Springer, The Netherlands, pp. 207–220.

Kesavan, J., Schepers, D., and McFarland, A. (2010). Sampling and Retation Efficiencies of Batch-Type Liquid Based Bioaerosol Samplers. *Aerosol Sci. Technol.* 44(10):817–829.

Lighthart, B., and Shaffer, B. T. (1995). Airborne Bacteria in the Atmospheric Surface Layer: Temporal Distribution Above a Grass Seed Field. *Appl. Environ. Microbiol.* 61(4):1492–1496.

Lin, X., Willek, K., Ulevicius, V., and Grinshpun, S. (1997). Effect of Sampling Time on the Collection Efficiency of All-Glass Impingers. *Am. Ind. Hygiene Assoc. J.* 58(7):480–488.

Samuels, A. C., Santarpia, J. L., Bottiger, J. R., Hunter, S., and Stuebing, E. W. (2006). Test Methodology Development for Biological Agent Detection Systems. *Proc. of SPIE.* 6378:6378–02–378–09.

Santarpia, J. L., Cunningham, D., Gilberry, J., Kim, S., Smith, E. E., Ratnesar-Shumate, S., and Quizon, J. (2010). Transport and Characterization of Ambient Biological Aerosol Near Laurel, MD. *Biogenetics Discuss*. 7:6725–6747.

Schroder, K. L, Hargin, P. J., Schmitt, D. J., Rader, D. J., and Shokair, I. R. (1999). Development of an Unattended Ground Sensor for Ultraviolet Laser-Induced Fluorescence Detection of Biological Agent Aerosols. *Proc. of SPIE.* 3855:82–91.

Semler, D. D., Roth, A. P., and Semler, K. A. (2004). Simulated Field Trials Using an Indoor Aerosol Test Chamber. *[Working paper no. A096944.]*. DyCOR Technologies LTD, Edmonton.

Shaffer, B. T., and Lighthart, B. (1997). Survey of Culturable Airborne Bacteria at Four Diverse Locations in Oregon: Urban, Rural, Forest, and Coastal. *Microb. Ecol.* 34(3):167–177.

Tilley, R. I., Ho. J., and Eamus. D. (2001). Background Bioaerosols and Aerosols at Two Sites in Northern Australia: Preliminary Measurements. *National Technical Information Service-Defense Technical Information Center.* DTSO-TR-1203.

United Stated Army Environmental Hygiene Agency. (1994). *Final Report: Kuwait Oil Fire Health Risk Assessment No. 39–26-L192–91*. Aberdeen Proving Ground, MD.

Vanderberg, L. A. (2000). Detection of Biological Agents: Looking for Bugs in All the Wrong Places. *Appl. Spectrosc.* 54(11):376A–385A.

Wilson, G. A., and Brady, J. (2004). Design Consideration and Signal Processing Algorithms for Laser-Induced Fluorescence Airborne Pathogen Sensors. *Proc. of SPIE.* 5617:1–13.

Wilson, G. A., and DeFreeze R. K. (2003). Autofluorescence Detection Using UV Diode Laser Simultaneous Excitation of Multiple Wavelengths. *Proc. of SPIE.* 5071:253–263.